# Finding A Volume Ratio of Hyaluronic Acid to Phe-Arg-Poly(ester amide)s to Form Drug-Delivering Nanoparticle Micelles

and

Preliminary Drug Loading Results

A Thesis

Presented to the Faculty of the Graduate School

of Cornell University

In Partial Fulfillment of the Requirements for the Degree of

Master of Science

by

Huahua Wan

December 2018

# ABSTRACT

Pseudo-protein is  a name used to describe an amino acid based poly(ester amide)s (aa-PEA). One possible application of pseudo-protein is as a drug delivery coating. To form a drug-delivery micelle, positively charged Phenylalanine-Arginine-PEA (Phe-Arg-PEA) was mixed with negatively charged hyaluronic acid (HA). HA, a natural polysaccharide abundant in human skin and the extracellular matrix, binds to the CD44 glycoprotein receptor on surface of cancer cells and is therefore a possible pathway to the  development of  precisely targeted cancer treatments. Nanoparticle micelles with smaller diameters are more efficient in the drug delivery process. In this study we attempted to find and adjust the ratio of hyaluronic acid to Phe-Arg-PEA to form nanoparticles of optimized size. Preliminary data on drug loading capability of sample ratio 3:2 were also summarized.

## BIOGRAPHICAL SKETCH

Jenny-(Huahua Wan) was born in China. She graduated with a BS from the Interdisciplinary Program of Life and Environmental Sciences in the University of Tsukuba, Japan. She did research in chemical biology under the supervision of Dr. Fukamizu and with the help of Dr. Hirota for one and a half year. During her stay in Ithaca, NY, she was attempting to study chemistry.

# ACKNOWLEDGMENTS

I want to thank my supervisor, Dr. David B. Zax for leading me through the whole process of learning in Ithaca. I also want to thank the DSG of the Department of Chemistry and Chemical Biology, Dr. H. Floyd Davis, and the program coordinator, Pat Hine for their support and help in navigation through the Master's Degree Program. The idea that this work might be a central portion for degree was an unexpected result of attending the class Human Body Repair taught by Dr. Chih-Chang Chu, who was also magnanimous in accepting me to observe and practice experiments in his lab.

TABLE OF CONTENTS

LIST OF FIGURES & TABLES

# LIST OF ABBREVIATIONS

HA: hyaluronic acids

AA-PEA: amino acid-based poly(ester amide)s

Phe-Arg-PEA: phenylalanine-arginine-poly(ester amide)s

GA: gambogic acids

# PREFACE

To complete the degree, this work was started and completed in the fall semester, 2018. I usually visited the lab two to three times between classes during workdays and one time on weekends. It was a delightful time for me doing the experiments and discussing with the postdoc in the lab.

# CHAPTER 1 – INTRODUCTION

## *INTRO TO THE MECHANISTIC BACKGROUND SUPPORTING THIS WORK*

Nanoparticle micelles encapsulate drugs and deliver them to cancer cells through the blood stream. This work reports initial efforts at producing encapsulations using a synthetic AA-PEA (also known as a "pseudo-protein") in Professor Chu's lab. The choice of Phe-Arg-PEA is convenient as it provides an easy way to provide positive charges (on the guanidinyl side chains of Arg) which will be useful to interact with the anionic HA When these two long-chain molecules are mixed in solution the counterbalancing charges allow them to intimately interact and under proper conditions to form a nanoparticle micelle. While the resulting nanoparticle micelle is schematically represented as double layered (Supplement 1) but realistically a sphere with three or more mingled layers. In the future, the micelles should be tested on crosslinking, stability, toxicity *in vitro*, and so on. (Figure 1)

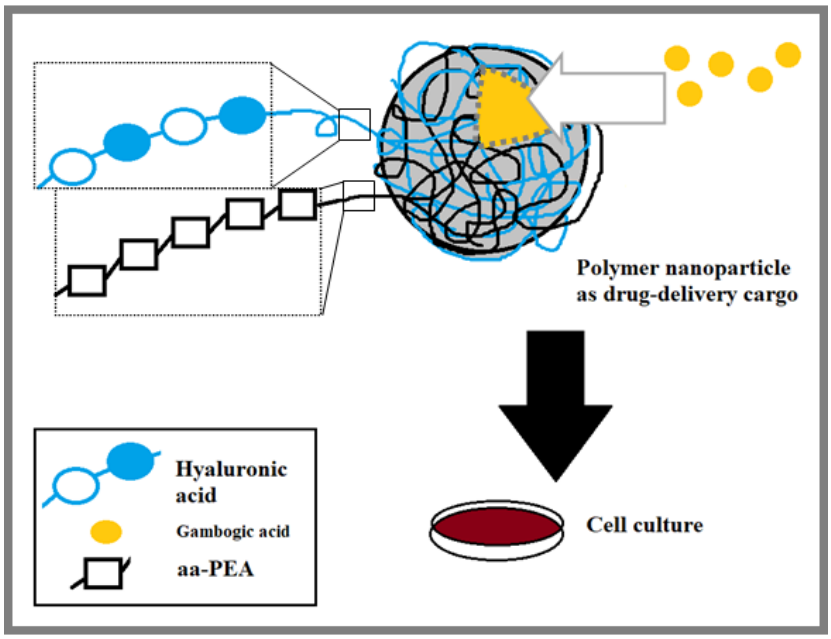


Figure 1. Mechanism of drug delivery by HA-Phe-Arg-PEA.

***AN INTRODUCTION TO AA-PEA***

AA-PEAs are biodegradable amino acid-based poly(ester amide)s synthesized from polymerization of different amino acids, diacids, diesters, or diols (Fig. 2) Theoretically any amino acid could be chosen as a component, which enables a big pool of upgradable products. Possible merits of specific choices are discussed in what follows, from its analogous role to proteins in human body, which will also clarify why we choose to refer to this class of artificial bio-inspired polymers as pseudo-proteins.

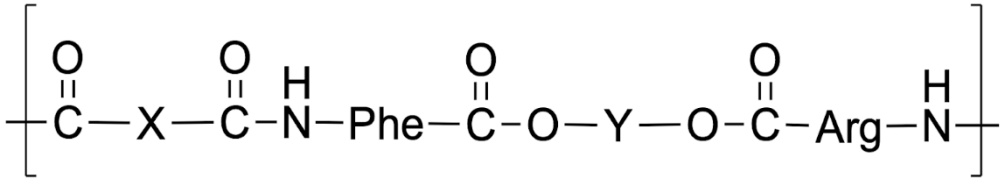


Figure 2. The chemical structure of the repeating unit of an example pseudo-protein, Phe-Arg-Poly(ester amide). Amino acids, diacids (Y), diols (X), amide bonds, and ester bonds are the main components in an aa-PEA, as defined by Chu.

**Pseudo-proteins and pseudo-protein-properties**

One essential similarity is that our PEA's are enzyme-degradable. Normal peptides are individual amino acids covalently linked through amide bonds. aa-PEA is distinctive in that within one repeating unit there are two amino acids, both ester and amide bonds, diols and dicarboxylic acids. For example, in this study, the aa-PEA used is Phe-Arg-PEA. The ester and amide bonds are sites that are biodegradable by enzymes like alpha-chymotrypsin, just as what they do to normal proteins, and the remaining constituents can

be returned to the cellular matrix where they can activate biochemical processes including macrophages which benefit wound healing as well. This satisfies one important requirement--which is the non-toxic biocompatibility of a biomaterial.

AA-PEA can be synthesized with essentially any amino acids incorporated into the backbone chain. The common twenty amino acids, with side chains that are either charged, polar, and/or aromatic, offer a wide range of functionality which can be used to consciously design properties into the synthetic polymer. The ring in proline could provide spatial obstacle. The thiol in cysteine could offer the reactivity of cross-linking. In this study, arginine offers cationic affinity in the electrostatic self-assembly process of the synthetic micelles. The aromatic ring in phenylalanine could help establish a hydrophobic layer against drugs - at inner side of the synthetic micelles to avoid drug leaking or unsteady encapsulation in the process.

AA-PEA could provide advanced tumor or cancer cell targeted treatments. While surgery, radiation, or chemotherapy are costly in terms of time, energy or money, and at the same time burdening the whole body, aa-PEA could be used to develop a precise targeted therapy to the tumors cost-efficiently.

***WHY HYALURONIC ACID?***

Hyaluronic acid is a natural polysaccharide with repeating unit of two sugars, *D*-glucuronic acid and *N*-acetyl-L-glucosamine, linked through ß-1, 4 and ß-1, 3 (Fig. 3). It is conserved evolutionarily and abundant in the extracellular matrix, from prokaryotes to eukaryotes, and is usually present as a high molecular weight polymer ranging from kiloDaltons to hundreds of kiloDalton. In human bodies, 50-60% of total HA composes the dermis, epidermis (Prasad N.Sudha, 2014) (See Fig. 4) and exists in virtually all other connective tissues and fluids (Laurent, 1989).

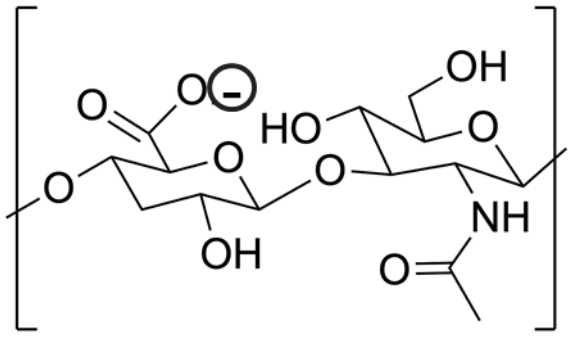


Figure 3. The chemical structure of the repeating unit of hyaluronic acid. The sugar on the left is glucuronic acid and the sugar on the right is acetylglucosamine. HA is usually present in large molecular weights, as in long random chains of huge number of repeating units.

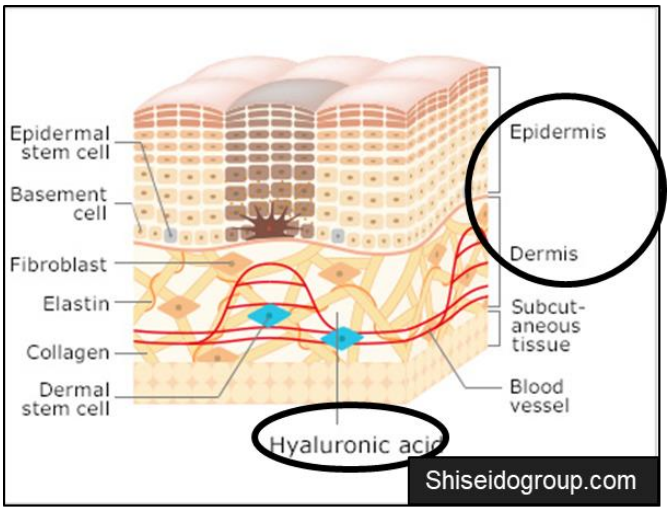


Figure 4. Location of HA in epidermis and dermis (circled) in human skin.

**HA has been widely exploited in cosmetics, tissue regeneration, and possibly other fields of human body repair.** As an elastic, hydrating, rejuvenating material, it is considered ideal for filling wrinkles and correcting scars on human bodies (Narins RS, 2003). Histological evidence *in vivo* was observed in rats, where non-animal-derived HA filler subcutaneously injected allowed ingrowth of tissue after fibroblast proliferation and migration, collagen formation, and growth of fat tissues. Hyaluronic acid can also be used to make synthetic hydrogels. In 2011 Prestwich fabricated a synthetic biograde ECM hydrogel as a clinical combination product after preparation using both microspinning and electrospraying techniques. The HA-based ECM was injected into rabbit femoral articular cartilage and was able to repair damages through enhancing endogenous natural repair mechanisms (D.Prestwich, 2011). In another study, one of the deviations of HA could repair spinal cord injury through cell delivery (Kubinova, 2018). Scientists modified HA into HA-hydroxyphenyl-RGD containing the integrin-binding peptide arginine-glycine-aspartic acid, and fibrinogen in the solution. Human stem cell-derived mesenchymal cells

were cultured and proliferated in this solution to spur growth as a treatment. Rats with hemisected vertabra subjected to the gel injection application were observed with migration of astrocytes, infiltration of newly generated blood vessels into the treatment area, and production of oligodendrocyte within it, the data of which shows a very promising future of a spinal cord injury repairing or restoration material.

**HA is involved in a variety number of physiological processes which appear linked to development of cancer cells.** In angiogenesis, the growth of new capillary vessels, HA specifically binds to the CD44 glycoprotein receptors which regulate the progression and metastasis of cancer cells on the surface of endothelial cells, and further stimulate their proliferation and migration (Linda T. Senbanjo and Meenakshi A. Chellaiah, 2017; J A P Gomes, 2004;D. C. West and S. Kurnar , 1989). HA also binds to the hyaluronan-mediated motility receptor HMMR (also known as CD168) which is a protein in breast tissue and potentially associated with BRAC1 and BRAC2 proteins in breast cancers in human bodies (NCBI, n.d.). Thus HA is involved in carcinogenesis and tumorigenesis as it is involved with both CD44 and CD168. The former has been shown to be a biomarker not just in breast cancer but in multiple other types of cancer cells, including in leukemia, pancreatic cancer, melanoma, prostate cancer, and others. HA's strong affinity for CD44 makes it a desirable component in building a precise nanoscale drug delivery cargo, which is the main reason why it was chosen in this study.

**In this study**, HA has been utilized as an outside coating layer of nanoparticles where the positive charged HA molecules in solution can form with aa-PEA electrostatically into a

micelle-like structure. Potential drugs inside the micelles could be delivered to cancer cells or tumor cells using this polymer nanoparticle cargo delivery, with the HA sheathing improving the access of the drug molecules to the cell interior as HA has complex rheological characteristics includes steady shear rates and relaxation time when expressed in different molecular sizes and concentrations (A. García-Abuín, 2011; Mathew Nicholls, 2018).

# CHAPTER 2

# MATERIALS AND METHODS

## *Materials*

**Hyaluronic acid** stored at 4 °C was dissolved in a mixed solution of Milli Q water and Dimethyl-sulfoxide (DMSO). Though HA dissolves in water alone, DMSO is added at ratio 1 : 1 v/v for better compatibility with the PEA to be added later. The solution was thoroughly stirred at room temperature after dissolution.

**Phe-Arg-PEA** was synthesized in C.C. Chu's lab. It was dissolved in DMSO before mixing with HA. Subsequently aa-PEA in DMSO solution was added into HA in 1:1 solution of water and DMSO (v/v), drop by drop while mixing and was fully stirred for at least one hour in the bench.

**Gambogic acid** was stored at -20 ℃ in solid form and dissolved in DMSO to 20 mg/ml prior to use. It is a potential anti-cancer candidate as it was found to possess anti-inflammatory effects in rats. GA also suppresses the mRNA expression of survivin. As survivin is a highly expressed marker of cancer and suppresses the apoptosis of cancer cells, GA's downregulation of its expression could have anti-cancer effects; in this work, its efficacy is not yet important as we are using it as a place-holder for whatever potential

drug might be developed. It was slowly added into newly mixed Phe-Arg-PEA solutions at room temperature before being mixed into HA solutions.

***Dialysis and filtration***

Well-mixed solutions with different portions of HA and aa-PEA were transferred into dialysis membrane sacks and were placed into a 1 L beaker filled with DI water. The water was stirred. By utilizing the principle of dialysis, DMSO would be extracted from the solutions in the sack and into the DI water in the beaker so as to achieve the balance of osmotic pressure across the membrane. While the molecules of DMSO are small enough to escape the porous membrane, the much larger aggregates of HA and aa-PEA polymers stay inside the membrane. The dialysis membrane was chosen from Thermo SnakeSkin™ Dialysis Tubing (10K MWCO). The dialysis process was carried out overnight, and underwent one or two times changes of water to thorough exchange DMSO out of the system. The extract was then vacuum-filtered to remove undissolved particles or random dust precipitated during the process.

Thermo SnakeSkin™ Dialysis Tubing (10K MWCO)

***Measurements of size and surface zeta potential***

Photo: Zetasizer Nano, CESI

Samples were analyzed using the Zetasizer Nano instrument in Cornell Energy Systems Institute. In Zetasizer Nano, sizes (d in nm) of the nanoparticles in suspended solutions were characterized based on Dynamic Light Scattering technique, where the laser shooting through solutions were collected by the avalanche photodiode detector and processed to generate a function of light intensity and molecular size. To ensure the results are within measuring criteria, sample solutions were filtered and checked before transferring into the optical cells. The surface zeta potential is potential gap across the electrical double layers of the nanoparticles was measured to demonstrate that the solutes are forming in an expected way without contaminations, usually in negative charge as the bigger portion of positively charged HA is in the solution. When the portion of HA is larger in the mix, zeta potential of the nanoparticles is expected to be negative. If not, there may not be adequate number of nanoparticles present in the mix.

***Measurement of drug loading percentage through ultraviolet absorbance***

Samples were adjusted to 1 M concentration, 1 ml volume before taken to measurement. By the light spectrometer, incident high energy UV light hit sample solutions in the transparent cell and transmitted light is measured. Using the Beer-Lambert law, percentage of sample drug loading were calculated from the trend line after UV absorbance was measured,

$$A = \varepsilon bC$$

$$\frac{A_{std}}{A_{sp}} = \frac{\varepsilon bC_{std}}{\varepsilon bC_{sp}}$$

$$\Rightarrow \frac{A_{std}}{A_{sp}} = \frac{C_{std}}{C_{sp}}$$

where $A_{std}$ is peak absorbance of UV (*a.u*).; ε is molar absorptivity of GA in *L mol/cm*; b is optical path distance in *cm*; $C_{std}$ stands for concentration of GA loaded in samples; and $C_{sp}$ represents wanted concentrations of GA loading of samples.

The standard curves were set to 5%, 25%, 40%, 50% and 75% (i.e. For the 5% standard curve, 50 µg GA powder was directly dissolved and vortexed in 1 ml solution with 1 : 1 v/v DMSO and $H_2O$, and so on). And the trendline of drug loading ratio (%) versus UV absorbance (nm) was approximated. Results were summarized in the table.

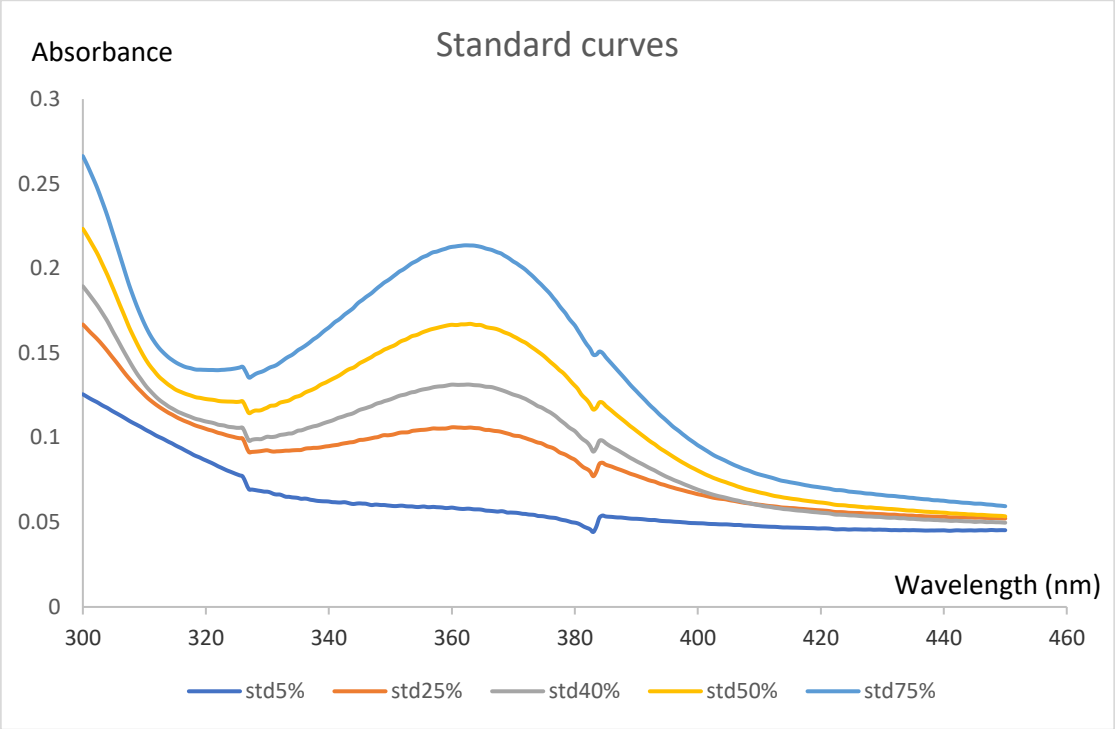


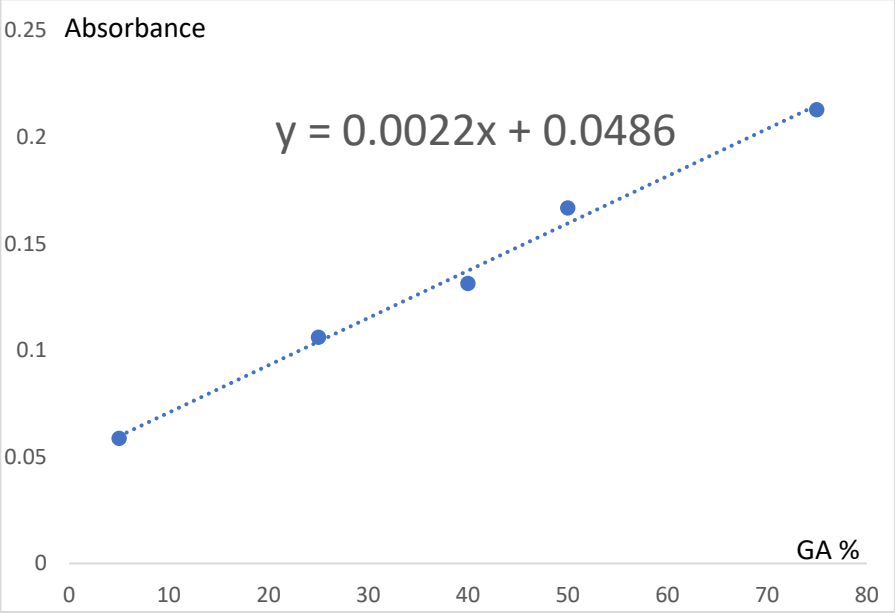


Figure 5, 6. Plot of standard curves and estimated linear correlation equation of GA% and absorbance. Theoretically the line of estimation should start from (0, 0) as the Beer-Lambert law shows direct proportionality between concentration and absorbance. The reasons for the small intercept at (0, 0.0486) could be improper calibration or instrumental

noise in practical. It was not the significant cause for the abnormal result in Table 4, where calculated drug% exceeded loaded drug% by 1.4%. As also explained in the result section, the error is highly possibly due to loss of Phe-Arg-PEA in the unstable drug-loading process where diameter of spheres were constantly changing.

# CHAPTER 3

# RESULTS AND DISCUSSIONS

## *Adjustment of HA-Phe-Arg-PEA ratios in the solutions*

A v/v ratio adjustment of HA to Phe-Arg-PEA was conducted first to see 1) If the synthesized Phe-Arg-PEA could form with HA under conducted experimental conditions; and 2) what ratio of HA : Phe-Arg-PEA would yield best results, which is a smallest diameter of the polymer nanoparticle. Data is shown in the following table.

Table 1. Measured diameters (D) and plot of sample 1-7 of different v/v ratios. (* see Figure 7)

| sp# | HA:PEA | D (nm) | Z pot. (mV) |
|---|---|---|---|
| 1 | 5:1 | 168.2 | -19.37 |
| 2 | 3:1 | 1419.0 | -28.07 |
| 3* | 3:1 | 157.4 | -14.77 |
| 4 | 2:1 | 197.3 | -22.7 |
| 5* | 3:2 | 138.7 | -18.9 |
| 6 | 1:1 | 206.5 | -20.7 |
| 7 | 1:3 | 419.6 | -15.6 |

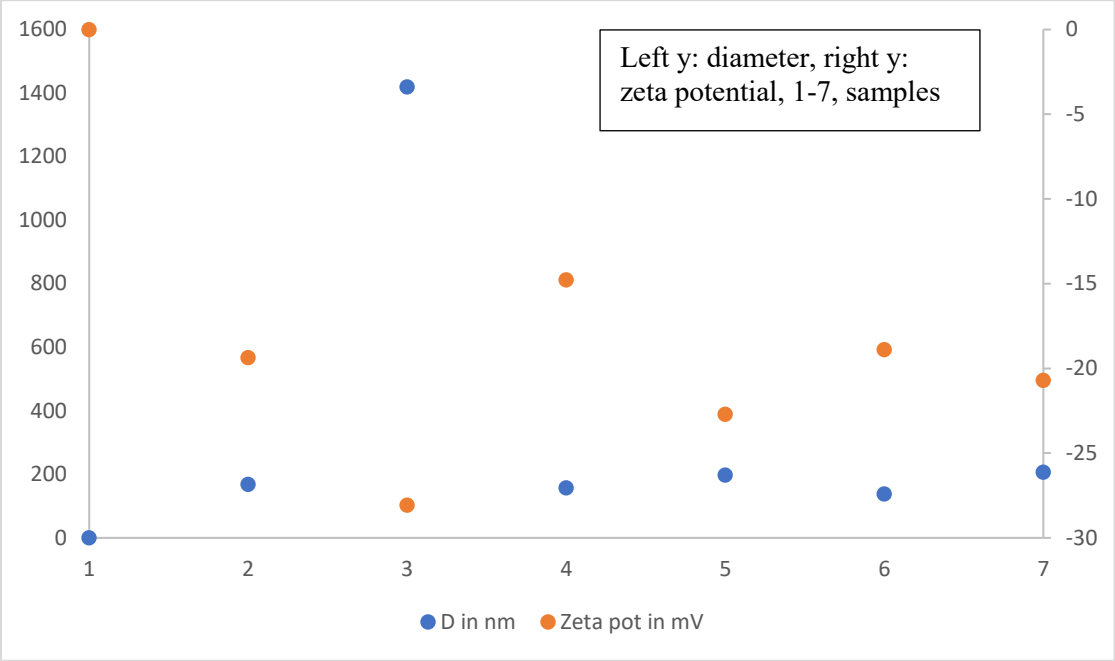


Figure 7. Measured diameters (D) and plot of sample 1-7 of different v/v ratios. (* conducted in different time to other samples; Clear graph of size intensity distributions of sample #5 3:2 is in supplement.)

From these results, sample 3:2 presented smallest diameters of polymer nanoparticles formed, while sample 3:1(sp# 2) had mostly undesired precipitations in the solution, whose diameters were ten times of usually expected ones, which should be due to contamination or mis manipulation. There was no obvious correlations between ratios with diameters or ratios with zeta potentials.

To continue testing its drug loading capability, GA was loaded this time with a percentage of 5%, 10%, and 15%, corresponding to 0.7 mg, 1.4 mg, and 2.1 mg in the table for a

longitudinal comparison of drug loading capability (Table 3). As explained in the methods, drugs successfully loaded could be measured by UV spectrometer (see Table 4).

Table 3. Third time results with extra GA drug loading

| **HA : PEA** | **HA (mg)** | **PEA (mg)** | **$H_2O$ (ml)** | **DMSO (ml)** | **Vtot (ml)** | **Mix. mg** | **Mix. conc. (M)** | **GA (mg)** | **Fin. conc. (M)** |
|---|---|---|---|---|---|---|---|---|---|
| **3:2** | 10 | 4 | 1 | 1.8 | 2.8 | 14 | 5 | 0.7 | 5.25 |
| | | | | | | | | 1.4 | 5.5 |
| | | | | | | | | 2.1 | 5.75 |

Table 4. UV absorbance, diameter, and zeta potential results of the samples in table 3 and calculated drug loading percentage using the Beer-Lambert Law from absorbance.

| [GA] in Sample 3 : 2 | GA (mg) | Abs. | Mass (µg) | Drug loading % | Size (nm) of first peak | Average size (nm) |
|---|---|---|---|---|---|---|
| 5% | 0.7 | 0.1240 | 34.265 | 3.40% | 194.4 | 1214 |
| **10%** | **1.4** | **0.3016** | **114.978** | **11.40%** | **124500** | |
| 15% | 2.1 | 0.1636 | 52.285 | 5.30% | 320.1 | 2230 |

From Table 4, overall speaking the first time drug loading process yielded unstable results. From the size results, there were all increase in particle diameters. However, according to supplement peak intensity graphs, there were polydiversities in all samples, which indicated during the 2 min measurement time in the machine, there was dynamic descending and merging of nanoparticles in the solutions.

It seems 10% GA in sample 3 : 2 yielded an abnormally large number after loading that was out of normal range, too different from data in sample 5% and 15%. Thus I suspect the

reasons could be unknown crystallization and thaw during lyophilization that unbalanced the system in some way. In Table 1 sample #2 (HA:PEA 3:1), there might be incomplete filtration. To avoid these, two layers of filter paper should be applied in filtration, and time of setting samples into vacuums could be shortened while keep samples on ice. And most importantly, handle the freeze drying process well, using multiple tubes for each sample.

***What to do in the future***

Besides those mentioned in the last section, in the future, larger total mass of samples should be used to confirm if there is variations on diameters. The same drug loading conditions in Table 3 & 4 should be set to sample of 1 : 1 for a horizontal comparison of it, as drug loading capability may not linearly relate to nanoparticle diameters.

Supplement 1. The ideal schematic structure of the synthetic polymer micelle nanoparticle, which has a double layer coating. The outer layer is the negatively-charged hyaluronic acid and the inner layer is the positively-charged Phe-Arg-PEA.

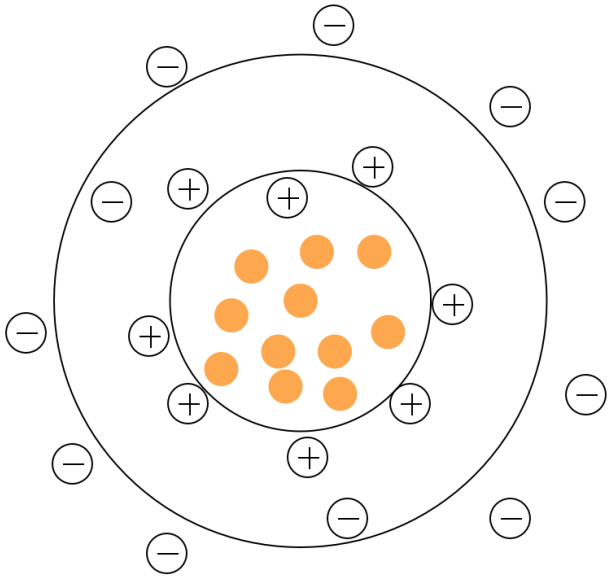

Supplement 2 (1): Size distribution graph of sample 3:2.

The polymer micelle was stably formed before drug loading as Peak 1 takes up 96% intensity. After drug loading, as in supplement 2 (2), (3), formed bigger polymer micelles were unstable and polydiversed. The graph result of drug loading 10% show no peaks at all. So it was not presented here.

| | | | |
|---|---|---|---|
| **Sample Name:** | 3-2 2 nov 1 | | |
| **SOP Name:** | mansettings.nano | | |
| **File Name:** | HAPEA23 Oct.dts | **Dispersant Name:** | Water |
| **Record Number:** | 38 | **Dispersant RI:** | 1.330 |
| **Material RI:** | 1.59 | **Viscosity (cP):** | 0.8872 |
| **Material Absorbtion:** | 0.010 | **Measurement Date and Time:** | Friday, November 2, 2018 2:53:46 ... |

| | | | |
|---|---|---|---|
| **Temperature (°C):** | 25.0 | **Duration Used (s):** | 70 |
| **Count Rate (kcps):** | 191.9 | **Measurement Position (mm):** | 3.00 |
| **Cell Description:** | Disposable micro cuvette (40µl) | **Attenuator:** | 9 |

| | | | **Size (d.nm):** | **% Intensity:** | **St Dev (d.nm):** |
|---|---|---|---|---|---|
| **Z-Average (d.nm):** | 142.1 | **Peak 1:** | 150.6 | 96.2 | 62.77 |
| **PdI:** | 0.291 | **Peak 2:** | 5080 | 3.8 | 562.7 |
| **Intercept:** | 0.934 | **Peak 3:** | 0.000 | 0.0 | 0.000 |
| **Result quality :** | Good | | | | |

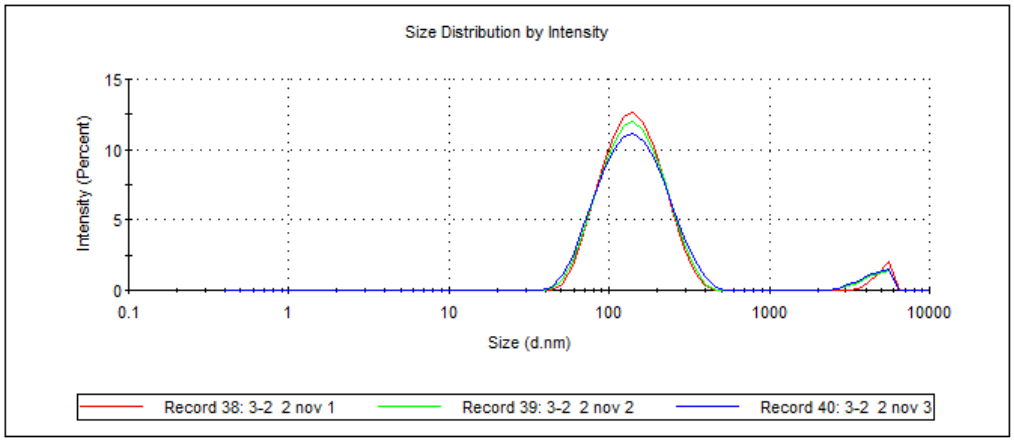

Supplement 2 (2): Size distribution graphs of sample 3:2 after 5% drug loading.

| | | | |
|---|---|---|---|
| **Sample Name:** | (1) 5% 1 | | |
| **SOP Name:** | mansettings.nano | | |
| **File Name:** | HAPEA 23 Oct.dts | **Dispersant Name:** | Water |
| **Record Number:** | 80 | **Dispersant RI:** | 1.330 |
| **Material RI:** | 1.59 | **Viscosity (cP):** | 0.8872 |
| **Material Absorbtion:** | 0.010 | **Measurement Date and Time:** | Thursday, November 29, 2018 2:51... |

| | | | |
|---|---|---|---|
| **Temperature (°C):** | 25.0 | **Duration Used (s):** | 70 |
| **Count Rate (kcps):** | 161.7 | **Measurement Position (mm):** | 3.00 |
| **Cell Description:** | Disposable micro cuvette (40µl) | **Attenuator:** | 9 |

| | | | **Size (d.nm):** | **% Intensity:** | **St Dev (d.nm):** |
|---|---|---|---|---|---|
| **Z-Average (d.nm):** | 1214 | **Peak 1:** | 194.4 | 100.0 | 16.22 |
| **PdI:** | 0.928 | **Peak 2:** | 0.000 | 0.0 | 0.000 |
| **Intercept:** | 1.12 | **Peak 3:** | 0.000 | 0.0 | 0.000 |

**Result quality :** Refer to quality report

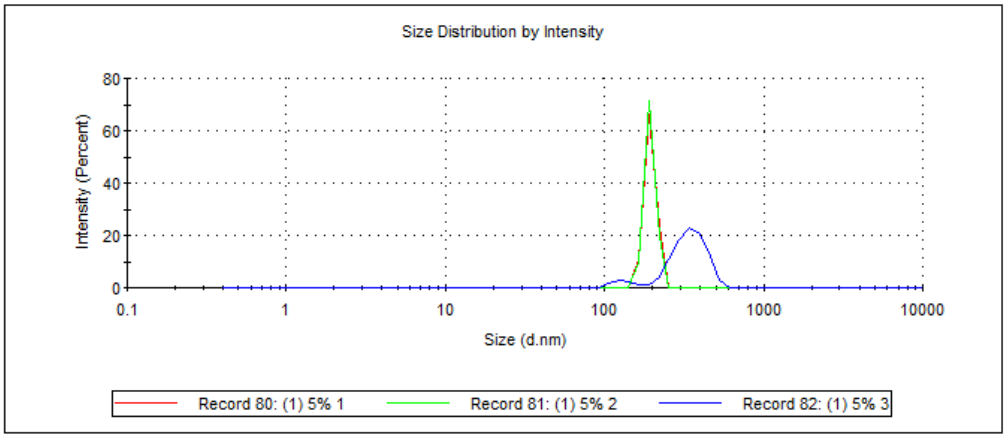

Supplement 2 (3): Size distribution graphs of sample 3:2 after 15% drug loading.

| | | | |
|---|---|---|---|
| **Sample Name:** | 15% 1 | | |
| **SOP Name:** | mansettings.nano | | |
| **File Name:** | HAPEA23 Oct.dts | **Dispersant Name:** | Water |
| **Record Number:** | 92 | **Dispersant RI:** | 1.330 |
| **Material RI:** | 1.59 | **Viscosity (cP):** | 0.8872 |
| **Material Absorbtion:** | 0.010 | **Measurement Date and Time:** | Thursday, November 29, 2018 3:20... |

| | | | |
|---|---|---|---|
| **Temperature (°C):** | 25.0 | **Duration Used (s):** | 60 |
| **Count Rate (kcps):** | 159.8 | **Measurement Position (mm):** | 3.00 |
| **Cell Description:** | Disposable micro cuvette (40µl) | **Attenuator:** | 7 |

| | | | **Size (d.nm):** | **% Intensity:** | **St Dev (d.nm):** |
|---|---|---|---|---|---|
| **Z-Average (d.nm):** | 2230 | **Peak 1:** | 320.1 | 100.0 | 23.30 |
| **PdI:** | 1.000 | **Peak 2:** | 0.000 | 0.0 | 0.000 |
| **Intercept:** | 1.16 | **Peak 3:** | 0.000 | 0.0 | 0.000 |

**Result quality :** Refer to quality report

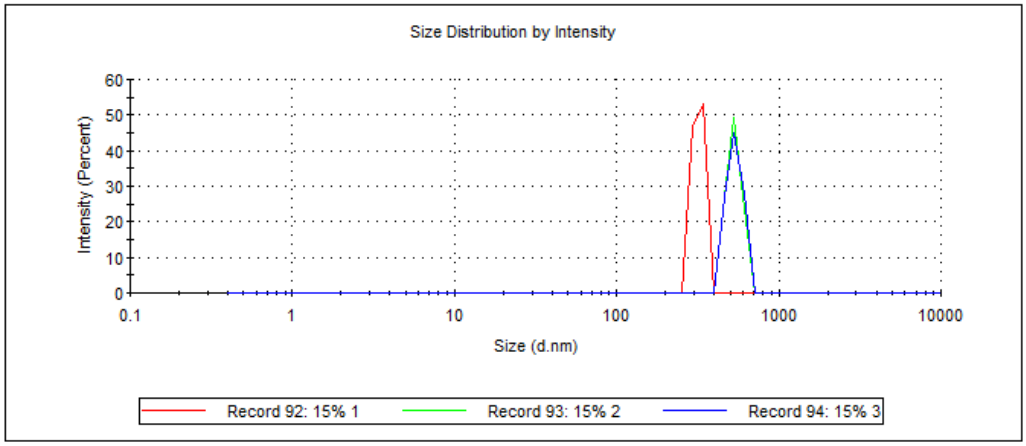

Works Cited

D. C. West and S. Kurnar . (1989). Hyaluronan and angiogenesis. *The biology of hyaluronan, Novartis Foundation Symposium* , 187-207.

D.Prestwich, G. (2011). Hyaluronic acid-based clinical biomaterials derived for cell and molecule delivery in regenerative medicine. *Journal of Controlled Release*, Volume 155, Issue 2, 193-199.

J A P Gomes, R. A.-R. (2004 ). Sodium hyaluronate (hyaluronic acid) promotes migration of human corneal epithelial cells in vitro. *Br J Ophthalmol. Jun;* , 88(6): 821–825.

J.R.E. FRASER, T. L. (1997). Hyaluronan: its nature, distribution, functions and turnover. *Journal of Internal Medicine*, 242: 27–33.

Kubinova, K. Z. (2018). Injectable hydroxyphenyl derivative of hyaluronic acid hydrogelmodified with RGD as scaffold for spinal cord injury repair. *Journal of Biomedical Materials Research*, Volume 106, Issue 4: p1129-1140.

Laurent, J. R. (1989). Turnover and metabolism of hyaluronan. *The biology of hyaluronan, Novartis Foundation Symposium* , p 41-59 .

Linda T. Senbanjo and Meenakshi A. Chellaiah. (2017). CD44: A Multifunctional Cell Surface Adhesion Receptor Is a Regulator of Progression and Metastasis of Cancer Cells. *Front Cell Dev Biol.* , 5: 18.

Mathew Nicholls, A. M. (2018). Rheological Properties of Commercially Available Hyaluronic Acid Products in the United States for the Treatment of Osteoarthritis Knee Pain. *Clinical Medicine Insights: Arthritis and Musculoskeletal Disorders*, Volume 11: 1-5.

Narins RS, B. F. (2003). A randomized, double-blind, multicenter comparison of the efficacy and tolerability of Restylane versus Zyplast for the correction of nasolabial folds. *Dermatol Surg*, 29:588–595.

Prasad N.Sudha, M. H. (2014). Beneficial Effects of Hyaluronic Acid. *Advances in Food and Nutrition Research*, Volume 72 Pages 137-176.